

# Quantum and semiclassical analysis of long-range Rydberg molecules

Brian E. Granger, Edward L. Hamilton, and Chris H. Greene  
*Department of Physics and JILA, University of Colorado, Boulder, Colorado 80309-0440*  
 (Received 9 March 2001; published 17 September 2001)

A recent study suggests the existence of highly polar and nonpolar long-range Rydberg molecules under temperature and density conditions representative of those found in atomic Bose-Einstein condensates. The electronic wave functions of these Rydberg molecules are characterized by an elliptically shaped nodal structure. We use a combination of quantum and semiclassical methods to explore this unique nodal structure and its correlations with the Born-Oppenheimer potential curves of the molecules. We demonstrate a special “quasiseparability” that arises in elliptic coordinates at certain internuclear separations and give a semiclassical interpretation of this in terms of quantized Einstein-Brillouin-Keller orbits.

DOI: 10.1103/PhysRevA.64.042508

PACS number(s): 31.50.Df

## I. INTRODUCTION

Rydberg states of long-range  $\text{Rb}_2$  molecules predicted in a recent study [1] exhibit several striking features. First, the Born-Oppenheimer potential curves oscillate as a function of internuclear separation  $R$  out to distances of at least  $10^2 - 10^4$  Bohr radii. Second, some of these molecular Rydberg states possess large electric dipole moments of magnitude  $D \approx R - (1/2)n^2$  a.u., where  $n$  is the principal quantum number of the Rydberg state. Third, the electronic wave functions of these Rydberg molecules have elliptically shaped nodal patterns, whose evolution with  $R$  is highly correlated with the oscillating potential curve.

These long-range molecules stand in contrast to more familiar homonuclear diatomic molecules having bond lengths of a few Bohr radii and no permanent electric-dipole moments. Given these differences, it is desirable to have a more complete understanding of the physics of these molecules. The current paper focuses on one aspect of the molecular physics, namely, the electronic wave function and its relation to the oscillations in the Born-Oppenheimer potential curves.

We develop a simple picture of these molecules using two ingredients: Rydberg states of atomic hydrogen, and the attraction between a slow electron and a ground-state Rb atom. At first glance, the molecular states seem to have little in common with atomic Rydberg states. However, a transformation to elliptic coordinates shows that most of the molecular physics is governed by highly excited atomic states. This transformation to elliptic coordinates also allows for semiclassical interpretations of these states.

Section II discusses the qualitative features of the electronic wave function and Born-Oppenheimer potential curves of these Rydberg molecules. Particular emphasis is placed on the evolution of the electronic states as the internuclear separation is changed. Section III shows how many of the qualitative features can be understood by solving the relevant Schrödinger equation in elliptic coordinates. In Sec. IV, the underlying simplicity of the quantum-mechanical solutions is reproduced and interpreted using semiclassical methods.

## II. QUALITATIVE FEATURES

We begin by recapitulating the qualitative features of the electronic wave functions and Born-Oppenheimer potential

curves. The relevant physics is that of a highly excited Rb atom ( $n \approx 30$ ) in the presence of a second, ground-state Rb atom a distance  $R$  (we use atomic units unless otherwise stated) away. The main features discussed in this paper are shown in Figs. 1 and 2, which show the Born-Oppenheimer potential curve and electronic wave function as a function of internuclear separation.

Most importantly, the nodal pattern of the electronic wave function is elliptically shaped. More specifically, the approximate nodal lines lie on confocal ellipses and hyperbolas characteristic of elliptic coordinates [2]. This is surprising because the Born-Oppenheimer Hamiltonian [Eq. (3.1)] is approximately separable in a number of coordinate systems (spherical, parabolic, elliptic). Why a strong elliptic character (rather than spherical, parabolic, or otherwise) emerges in the

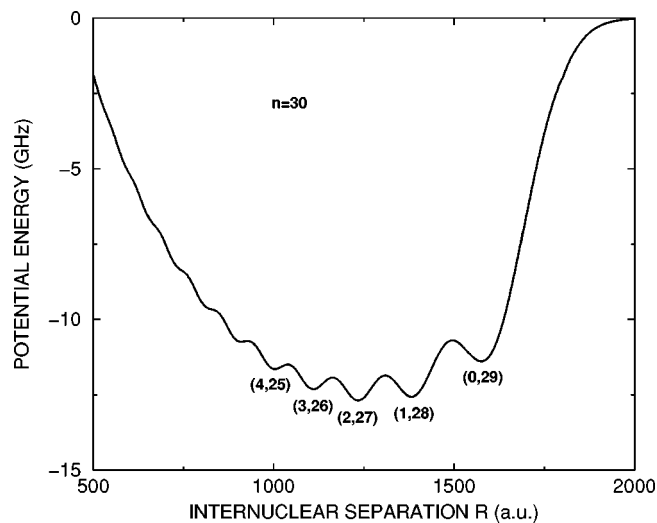


FIG. 1. Born-Oppenheimer potential curve for a highly polar  $n=30$  Rydberg state of  $\text{Rb}_2$ . The electronic wave function associated with this potential (see Fig. 2) shows striking elliptically shaped nodal patterns. The approximate numbers of nodes in the electronic wave function ( $\nu_\xi, \nu_\eta$ ) are shown below each minima. Note that the effective quantum numbers ( $\nu_\xi, \nu_\eta$ ) evolve continuously as a function of internuclear separation, but are integer valued at the minima. This paper gives quantum and semiclassical interpretations of the oscillating potential curve and associated wave function.

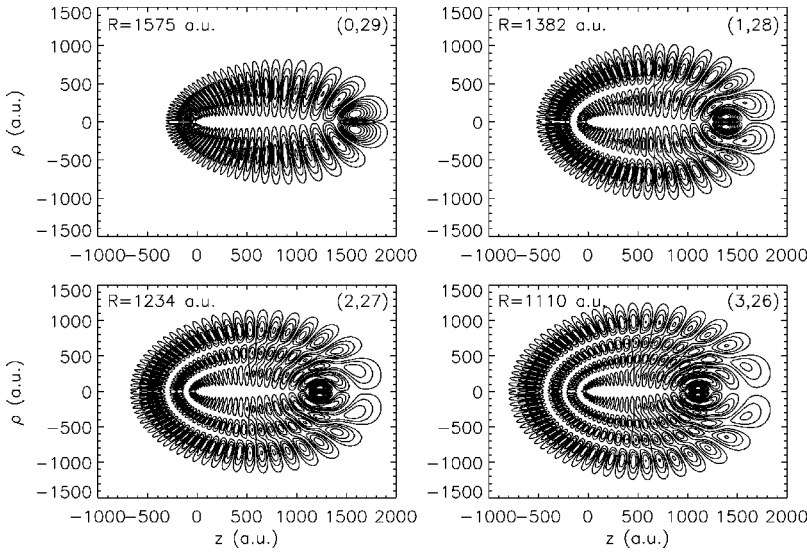


FIG. 2. Contour plots of  $\rho|\Psi(\rho,z)|^2$  of the Born-Oppenheimer wave functions of a long-range  $\text{Rb}_2$  molecule at the energy of an  $n=30$  Rydberg state. Four internuclear separations are shown ( $R=1575,1382,1234,1110$ ) corresponding to the outermost minima in the oscillating potential curve (see Fig. 1). These states are labeled by the approximate numbers of nodes ( $\nu_\xi, \nu_\eta$ ) in the two elliptic directions. Although the nodal lines are not exact, the strong antinodes make this labeling useful. The characteristic elliptically shaped nodal pattern is preserved as the nuclei get closer together, but the number of nodes in the two elliptic directions get redistributed from the angular  $\eta$  direction to the radial  $\xi$  direction as the internuclear separation is decreased.

molecular states is not initially obvious. Notice, secondly, that the numbers of approximate nodes in the two elliptic directions (radiuslike  $\xi$  and anglelike  $\eta$ ) are constrained by the principal quantum number  $n$  of the unperturbed electron. We use effective quantum numbers in elliptic coordinates ( $\nu_\xi$  and  $\nu_\eta$ ) to count the approximate numbers of nodes in the molecular wave function. These effective quantum numbers are then constrained by the principal quantum number  $n$  through the relation

$$\nu_\xi(R) + \nu_\eta(R) = n - 1. \quad (2.1)$$

We think of  $\nu_\xi(R)$  and  $\nu_\eta(R)$  as *effective* quantum numbers because they depend continuously on the internuclear separation  $R$ . Again, this relationship is surprising because  $\nu_\xi$  and  $\nu_\eta$  characterize the full molecular state, whereas  $n$  contains information only about the unperturbed atomic Rydberg state of Rb. A third observation is that the nodal structure evolves in a highly constrained manner as the internuclear separation is changed. As the internuclear distance decreases, the nodes in the angular elliptic direction  $\eta$  disappear one by one, and are replaced by new nodes in the radial elliptic direction  $\xi$ . A final observation is that the nodal structure of the electronic wave function is strongly correlated to the oscillations in the Born-Oppenheimer potential curve. At the minima in the oscillating potential curve, the nodal structure separates cleanly, although still only approximately, into an integral number of excitations in the angular and radial elliptic coordinates. In other words, at the minima of the potential curve,  $\nu_\xi$  and  $\nu_\eta$  are integers.

As stated previously, Figs. 1 and 2 demonstrate these qualitative observations by showing the potential curve and electronic wave function for an  $n=30$  Rydberg state of  $\text{Rb}_2$  as a function of internuclear separation  $R$ . Figure 1 shows how the Born-Oppenheimer potential curve oscillates dramatically out to 1000's of a.u. The values of the effective quantum numbers ( $\nu_\xi, \nu_\eta$ ) of the molecular state are shown below each minima in the curve. Figure 2 shows contour plots of the electron probability density at selected minima ( $R=1575,1382,1234,1110$  a.u.) in the potential curve. The

elliptically shaped nodal structure is maintained as the internuclear separation is changed. At the outermost minimum ( $R=1575$ ) all of the nodes ( $n-1=29$ ) are in the angular  $\eta$  direction. At the next minimum ( $R=1382$ ) there is a single node in the radial  $\xi$  direction and one less in the  $\eta$  direction. This pattern of redistributing the nodes from the  $\eta$  direction to the  $\xi$  direction continues as the internuclear separation passes through the other minima ( $R=1234,1110$ , and so on) in the potential curve.

These are the basic qualitative features that this paper sets out to explore. The robust, elliptic nodal structure of the electronic states suggest that the problem will simplify in elliptic coordinates. Elliptic coordinates have been used to treat a number of other two center problems such as  $\text{H}_2^+$  [3] and hydrogen in the presence of a point dipole [4]. From this standpoint, it is no surprise that elliptic coordinates are useful for our current system. However, it is desirable to understand both why elliptic coordinates seem to be preferred in our system, and exactly how the description is simplified when elliptic coordinates are used.

### III. QUANTUM TREATMENT IN ELLIPTIC COORDINATES

The first method that we use to understand the apparent simplicity of the electronic wave functions is degenerate perturbation theory. To emphasize the simple nature of the electronic wave functions, we neglect the complications of both fine structure and the non-hydrogenic Rb ionic core. With this approximation, the Born-Oppenheimer Hamiltonian is a combination of the Coulomb attraction and a short-range interaction potential centered on the ground state Rb atom. Greene and coworkers [1,5] model this interaction using a Fermi pseudopotential, a Dirac  $\delta$  function of strength  $2\pi A_T[k(R)]$ , where  $A_T[k(R)]$  is the triplet scattering length for an electron-Rb encounter at wavelength  $k$ . The electronic Hamiltonian then has the particularly simple form

$$H = \frac{p^2}{2} - \frac{1}{r} + 2\pi A_T[k(R)]\delta(\vec{r} - \vec{R}). \quad (3.1)$$

At most wavelengths near zero energy, the scattering length  $A_T[k(R)]$  is negative. The long-range molecules discussed in this paper depend critically on this net attraction between the Rydberg electron and the ground-state Rb atom. As in Ref. [1], the energy-dependent  $A_T[k(R)]$  is calculated from its zero energy value  $A_T[0]$  [6] and the Rb( $5s$ ) polarizability [7] using a generalized quantum-defect theory [8]. The three-dimensional delta function potential is known [9] to give ill-behaved solutions of the Schrödinger equation. In spite of this, treating the delta function using perturbation theory is straightforward and gives sensible results. In the absence of the ground-state Rb atom, the Hamiltonian is just that of hydrogen, which is separable in a number of coordinate systems (spherical, elliptic, parabolic). Any of these coordinate systems can be used to define unperturbed eigenstates for use in perturbation theory. However, nondegenerate eigenstates based on any of these coordinate systems lead to the same elliptically shaped molecular states (Fig. 2) once the perturbation has been included. In the following sections, we carry out quantum and semiclassical calculations in elliptic coordinates to show how the molecular states acquire this robust elliptic character.

Guided by the elliptically shaped nodal patterns, we introduce elliptic coordinates, defined with the foci of the elliptical coordinate system placed on the ion (at the origin) and the perturbing Rb atom  $(\rho, z) = (0, R)$ . If  $r_1$  and  $r_2$  are the distances between the Rydberg electron and the two foci of our coordinate system, the elliptic coordinates are defined as

$$\xi = \frac{r_1 + r_2}{R}, \quad (3.2)$$

$$\eta = \frac{r_1 - r_2}{R}. \quad (3.3)$$

These coordinates are constrained to the ranges  $1 \leq \xi < \infty$  and  $|\eta| \leq 1$ . Next, our unperturbed elliptic eigenstates are introduced.

### A. Unperturbed elliptic states

The elliptic eigenstates we construct here are stationary eigenstates of the hydrogen atom. These states differ from the traditional states of hydrogen (eigenstates of  $H, \vec{L}^2, L_z$ ) through the replacement of  $\vec{L}^2$  by a constant of the motion that emerges out of elliptic coordinates. The Schrödinger equation for an electron (in a molecular  $\Sigma$  state) in a Coulomb potential in elliptic coordinates reads [10,2,11]

$$\left[ -\frac{1}{2} \frac{\partial}{\partial \xi} (\xi^2 - 1) \frac{\partial}{\partial \xi} - \frac{1}{2} \frac{\partial}{\partial \eta} (1 - \eta^2) \frac{\partial}{\partial \eta} - \frac{R}{2} (\xi - \eta) - \frac{R^2}{4} E (\xi^2 - \eta^2) \right] \Psi(\xi, \eta; R) = 0. \quad (3.4)$$

This equation separates into two one-dimensional eigenvalue problems for the elliptic separation constant  $B(R)$

$$\left[ -\frac{1}{2} \frac{\partial}{\partial \xi} (\xi^2 - 1) \frac{\partial}{\partial \xi} - \frac{R}{2} \xi - \frac{R^2}{4} E \xi^2 \right] F(\xi, R) = B(R) F(\xi, R), \quad (3.5)$$

$$\left[ -\frac{1}{2} \frac{\partial}{\partial \eta} (1 - \eta^2) \frac{\partial}{\partial \eta} + \frac{R}{2} \eta + \frac{R^2}{4} E \eta^2 \right] \Phi(\eta, R) = -B(R) \Phi(\eta, R), \quad (3.6)$$

where  $\Psi(\xi, \eta; R) = F(\xi, R) \Phi(\eta, R)$ . Given a total energy  $E = -1/2n^2$  and a distance  $R$ , the separation constant  $B(R)$  becomes quantized when boundary conditions appropriate for bound states are imposed. We label these states by the number of nodes in the  $\xi$  direction,  $n_\xi = (0, \dots, n-1)$ . The number of nodes in the angular  $\eta$  direction is then given by the constraint

$$n_\eta = n - 1 - n_\xi. \quad (3.7)$$

While this constraint resembles that of the full molecular eigenstates (2.1), at this point,  $n_\xi$  and  $n_\eta$  are integers characterizing the primitive atomic states and they do not depend upon the parameter  $R$ . However, when we use these primitive eigenstates to construct the molecular state, the  $R$ -dependent molecular relationship (2.1) will emerge out of the atomic one (3.7).

Although analytical power series solutions of these Eqs. (3.5), (3.6) have been found [2,10,11], an efficient way of calculating the solutions is to diagonalize the one-dimensional Hamiltonians in a  $B$ -spline basis set. This procedure produces the elliptic Coulomb states  $\Psi_{n_\xi}(\xi, \eta; R)$  along with the corresponding values of the separation constant  $B_{n_\xi}(R)$ . In all of the preceding equations, the internuclear separation  $R$  appears as a continuous parameter. However, these equations do not yet include the effect of the perturbing Rb atom. So far, the parameter  $R$  only gives the distance between the foci of our elliptic coordinate system.

At least back to Sommerfeld [12], it has been known that the hydrogen atom is separable in elliptic coordinates. Although the separability of the hydrogen atom in elliptic coordinates is not widely known, a number of authors have investigated the properties of the elliptic eigenstates. Erikson and Hill first [13] showed that the elliptic separation constant  $B(R)$  was related to the orbital angular momentum about the two foci of the coordinate system (see also Refs. [3,14]). In Sec. IV, we give a lesser known form [15] of this constant of the motion in terms of the angular momentum  $L^2$  about one focus, and the projection of the Runge-Lenz vector  $\vec{A}$  onto the internuclear axis. Analytical solutions of the one-dimensional Hamiltonians (3.5), (3.6) have been given [2,11] in terms of the associated Legendre polynomials. A more recent work of Sung and Herschbach [11] gives a thorough discussion of the elliptic eigenstates and their relation to the more traditional spherical eigenstates. In spite of this previous work, we feel that the striking nature of the elliptic states of hydrogen has not been fully appreciated. For our purposes, the most important features are elucidated in two-dimensional contour plots of the electron probability density of these states. Figure 3 shows contour plots of the electron

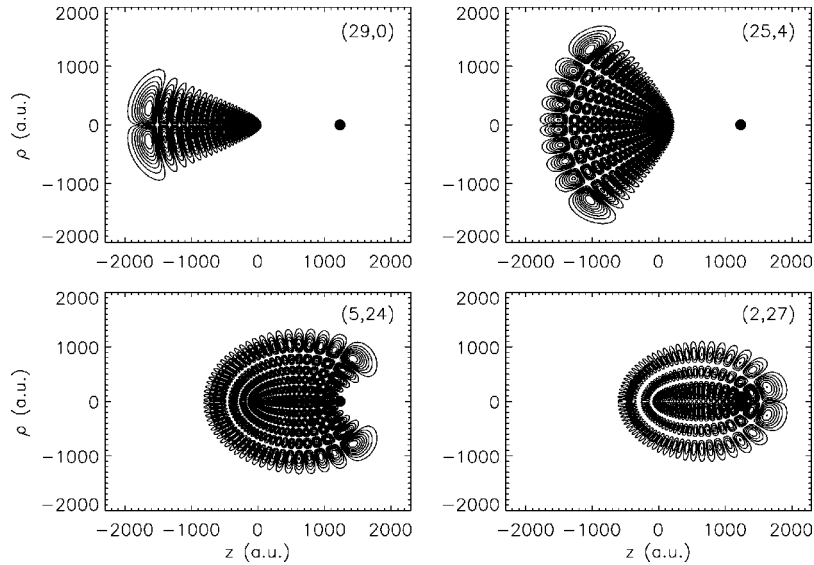


FIG. 3. Examples of elliptic eigenstates of the  $n=30$  hydrogen atom defined with an elliptic coordinate system where the distance between the foci of the coordinate system is 1232 a.u. The foci of the coordinate system have been placed at the origin and at  $(\rho, z) = (0, 1232)$  (shown by a small circle). These stationary states of hydrogen have large permanent dipole moments and striking nodal patterns. While the states are constructed in elliptic coordinates, the probability density  $\rho|\Psi(\rho, z)|^2$  is shown in cylindrical coordinates for clarity. The states are labeled by the numbers of nodes in the  $\xi$  and  $\eta$  directions,  $(n_\xi, n_\eta)$ . Shown are the (29,0) (upper left), (25,4) (upper right), (5,24) (lower left), and (2,27) (lower right) states. While the physics of the perturbing Rb atom is not included in these states, in the next section, the ground-state Rb atom will be placed at the second foci (small circle) of the coordinate system. It is clear that only the states having an elliptically shaped nodal pattern, such as the (2,27) state, will have any overlap with the perturbing Rb atom.

probability density for four of the degenerate elliptic states in the  $n=30$  manifold. The value of  $R$  for the elliptic coordinates underlying these states is 1232 a.u. These contour plots show that many of these states have large permanent electric-dipole moments. To our knowledge, the unusual nodal patterns of these states, which range from elliptical (0,29) to semicircular (14,15) to wedge (29,0) shaped, have not been reported in the literature thus far. Next, these states are used as zero-order eigenstates in perturbation theory.

### B. Degenerate perturbation theory

To include the effect of the perturbing Rb atom, the perturbation is diagonalized in the basis of elliptic eigenstates. The relevant perturbation matrix is

$$V_{n_\xi n'_\xi}(R) = 2\pi A_T[k(R)] \langle n_\xi | \delta(\vec{r} - \vec{R}) | n'_\xi \rangle. \quad (3.8)$$

Because this matrix is separable, only one state splits away from the degenerate  $n$  manifold when it is diagonalized. The total energy of the state can be found analytically, and is given by the expression

$$\begin{aligned} E_n(R) &= \frac{-1}{2n^2} + \sum_{n_\xi} |V_{n_\xi n_\xi}(R)|^2 \\ &= \frac{-1}{2n^2} + 2\pi A_T[k(R)] \sum_{n_\xi} |\Psi_{n_\xi}(1,1;R)|^2, \end{aligned} \quad (3.9)$$

which is used in Fig. 1 to calculate the Born-Oppenheimer potential curve. The wave function is then a linear combination of the elliptic eigenstates  $\Psi_{n_\xi}(\xi, \eta; R)$

$$\Psi_n(\xi, \eta; R) = \sqrt{2\pi |A_T[k(R)]|} \sum_{n_\xi} \Psi_{n_\xi}(1,1;R) \Psi_{n_\xi}(\xi, \eta; R). \quad (3.10)$$

It is clear that both the Born-Oppenheimer potential curve (3.9) and wave function (3.10) are determined by the values of the primitive elliptic eigenstates  $\Psi_{n_\xi}(1,1;R)$  at the position of the perturbing Rb atom  $(\xi, \eta) = (1,1)$ . In general, the wave functions and eigenvalues include contributions from all  $n$  elliptic eigenstates in the degenerate manifold. That the molecular states show a strong elliptic character is seen when the values  $\Psi_{n_\xi}(1,1;R)$  are shown as a function of internuclear separation  $R$ . Figure 4 shows a plot of the values of  $|\Psi_{n_\xi}(1,1;R)|^2$  ( $n_\xi = 0, \dots, 10$ ) for an unperturbed  $n=30$  state as a function of  $R$ . At certain internuclear separations, a single primitive elliptic state dominates the molecular wave function (3.10) and Born-Oppenheimer potential curve (3.9). A comparison between the coefficients in Fig. 4 and the Born-Oppenheimer potential curve in Fig. 1 shows that the minima in the potential curve occur precisely where a single elliptic state is dominating the molecular wave function. This “quasiseparability” of the full wave function means that at certain internuclear separations, the full Hamiltonian (including the perturbation) is nearly diagonal in the basis of primi-

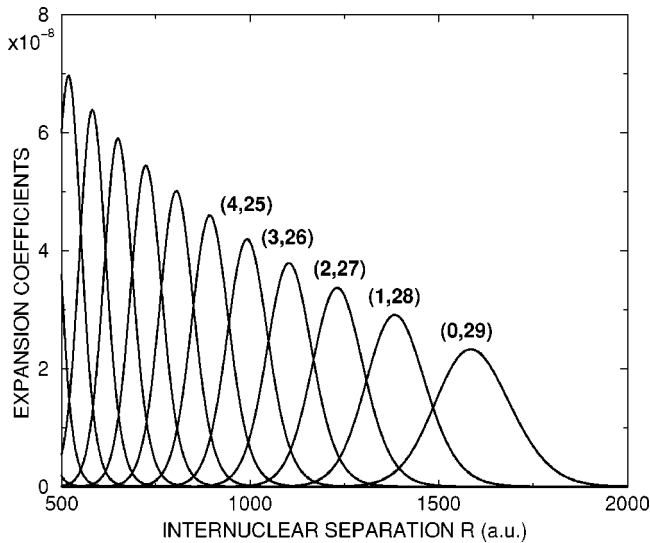


FIG. 4. The values of the expansion coefficients  $|\Psi_{n_\xi}(1,1;R)|^2$  for an  $n=30$  state. These coefficients determine which elliptic eigenstate of hydrogen (see Fig. 3) dominates the molecular wave function and Born-Oppenheimer potential curve (Figs. 1 and 2) at a given radius. Because the Born-Oppenheimer potential curve is simply  $2\pi A_T[k(R)]$  times the sum of all the coefficients in this figure, the minima in the potential curve coincide with the radii where the contribution of a single elliptic state is dominant. Each peak in the graph is labeled by the elliptic quantum numbers  $(n_\xi, n_\eta)$  of the state the peak represents. The quasiseparability occurs at internuclear separations where the coefficient of a single elliptic state dominates.

tive elliptic eigenstates. In some sense, the potential energy is minimized when the amount a nonseparability in elliptic coordinates is the least.

Furthermore, as the internuclear separation is changed, the specific elliptic state that dominates the sums in Eqs. (3.10) and (3.9) changes. This accounts for the redistribution of the nodes in the molecular wave function from the  $\eta$  to the  $\xi$  direction as the internuclear separation decreases (see Figs. 1 and 2). Thus, at the outermost minimum ( $R = 1575$  a.u.), Fig. 4 shows a peak in the contribution of the  $n_\xi=0$  state. At the next minimum ( $R=1382$  a.u.), the  $n_\xi = 1$  state has come to dominate. As the character of the molecular state evolves from one elliptic state to another the numbers of nodes in the electronic wave function  $(\nu_\xi, \nu_\eta)$  evolve according to the constraint of Eq. (2.1). While this quantum analysis give us a qualitative picture as to why the constraint of Eq. (2.1) holds for the molecular states, Sec. IV provides a quantitative semiclassical derivation of the relation.

Thus, we have shown how an unexpected “quasiseparability” in elliptic coordinates emerges at certain internuclear separations. These special internuclear separations are precisely the minima in the Born-Oppenheimer potential curve. That the Born-Oppenheimer Hamiltonian is nearly diagonal in elliptic coordinates at a sequence of internuclear radii is an unexpected simplification that explains why the nodal structure of the molecular states is elliptically shaped. The evolution of the molecular state with internuclear separation can

be viewed as an change in the contributions of the primitive elliptic states that comprise the wave function. Now we turn to a semiclassical description of these states.

#### IV. SEMICLASSICAL ANALYSIS

Semiclassical methods permit a simple interpretation of multidimensional quantum systems [16]. In the absence of the perturbing Rb atom, the long-range dynamics of the Rydberg electron are purely Coulombic. Our main challenge is therefore to include the effect of the perturbing Rb atom in a semiclassical treatment. In principle, it would be possible to include the perturbing potential using classical perturbation theory [17]. Rather than this approach, we focus on a more qualitative viewpoint in this paper. In two different semiclassical approaches, we show that the effect of the perturber can be understood in terms of unperturbed Coulomb trajectories that are constrained to pass through the ground-state Rb atom. One way of thinking about this, is that the delta-function perturbation potential (3.1) can be viewed as a constraint on the relevant trajectories of the system. First, we give a semiclassical interpretation of the elliptically shaped nodal structure using a semiclassical Green’s function. Then we use ideas from semiclassical Einstein-Brillouin-Keller (EBK) quantization to show how much of the insight gained from quantum degenerate perturbation theory can be understood and interpreted in terms of classical trajectories that pass through the perturbing Rb atom.

##### A. Semiclassical Green’s function

The first way of including the effect of the perturbing Rb atom semiclassically is to replace its delta-function Fermi potential by an inhomogeneous delta-function source at the perturbing atom. While this is clearly an approximation, we show that this approximation reproduces the solutions from degenerate perturbation [Eq. (3.10)] theory extremely well. The resulting object of interest is then the Coulomb Green’s function with the source placed at the position of the ground-state Rb atom. The semiclassical Green’s function can be written [16] as a sum over classical trajectories that propagate from  $\vec{x}'$  to  $\vec{x}$  with energy  $E$

$$G(\vec{x}, \vec{x}', E) \approx \sum_{\text{tra}j} \sqrt{|A|} e^{iS(\vec{x}, \vec{x}', E) - i\mu\pi/2}.$$

For our purposes, the most important quantities in this expression are the classical action  $S(\vec{x}, \vec{x}', E)$  and the Maslov index  $\mu$  of each trajectory, which counts the numbers of sign changes of the amplitude  $A$ . The amplitude  $A$  is a measure of the stability of each classical path. If the energy  $E$  is fixed and the source coordinate of the Green’s function is set to be at the position of the perturbing atom ( $\vec{x}' = \vec{R}$ ) there are only four classical trajectories that contribute to the Green’s-function  $G(\vec{x}, \vec{R}, E)$ . These four paths always lie on two Kepler ellipses that intersect the points  $\vec{x}$  and  $\vec{R}$  and have a Coulomb potential at one focus. An example of these four paths is seen in Fig. 5. The foci of the elliptic coordinate system (the Coulomb singularity and the perturbing Rb

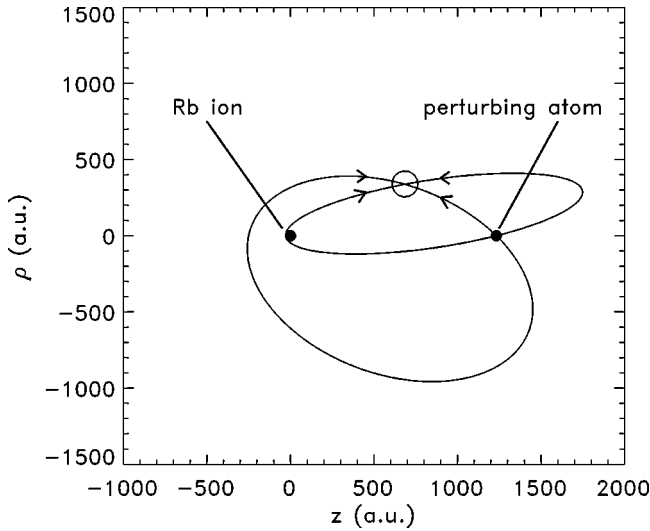


FIG. 5. An example of the four classical trajectories contributing to the semiclassical Green's function  $G(\vec{x}, \vec{R}, E)$ , at the energy of an  $n=30$  Rydberg state. The trajectories lie on two Kepler ellipses intersecting the perturber at  $\vec{R}$  (right solid circle) and the observation point  $\vec{x}$  (hollow circle). These ellipses are unique when one focus is constrained to be at the Coulomb singularity at the origin (left solid circle).

atom) are shown as solid circles. The Green's function is then a coherent sum of the four trajectories that propagate from the ground-state Rb atom to the observation point marked by a hollow circle.

Figure 6 shows contour plots of both the quantum and semiclassical Coulomb Green's function with the source point placed at the ground-state Rb atom  $(\rho, z) = (0, 1234)$ . The semiclassical Green's function has been constructed as described above, and shows strong agreement with the molecular wave function found using degenerate perturbation theory (Fig. 2) and the quantum Green's function also pictured here. The quantum Green's function shown in Fig. 6 is based on an analytical expression first derived by Hostler [18,19]. The good agreement of these three methods (quantum and semiclassical Green's function, and degenerate perturbation theory) show that the inclusion of the perturbing Rb atom through an inhomogeneous source term in the Schrödinger equation is a good approximation for the problem at hand. Additionally, from a semiclassical perspective, then, the nodal structure of these electronic wave functions is governed by two things. First, the long-range Coulomb physics provides the majority of the dynamical evolution. Second, the ground-state Rb atom at  $\vec{R}$  selects only Coulomb orbits that pass through this point. From this perspective, constraining the trajectories to pass through the ground-state Rb atom is a perfectly sensible way of including the effect of the perturbation in a semiclassical treatment. In the next section, we include this constraint on the trajectories in an EBK style analysis of the problem.

### B. Constrained EBK quantization

For integrable multidimensional Hamiltonians, the trajectories of the system are constrained to loop around invariant

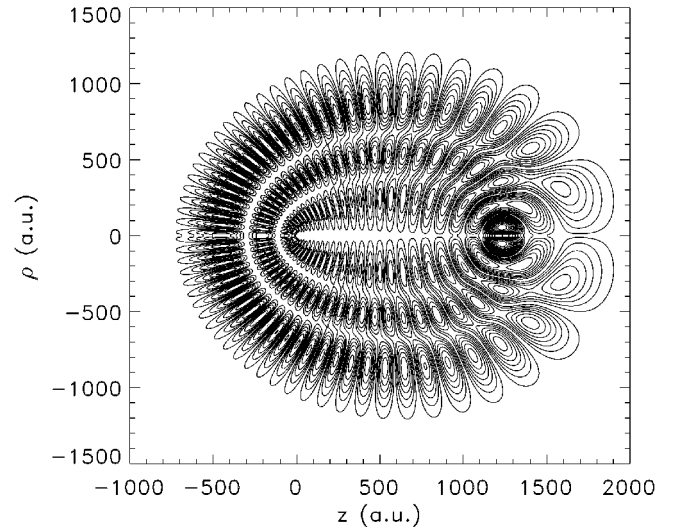
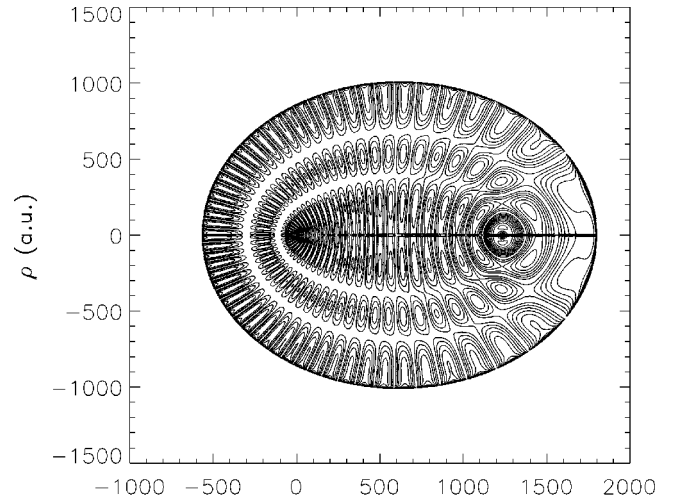


FIG. 6. Contour plot of the semiclassical (upper) and quantum (lower) Coulomb Green's function with the source coordinate placed at the ground-state Rb atom  $(\rho, z) = (0, 1234)$ . The Coulomb Green's function is relevant when the delta function perturbation potential is approximated by an inhomogeneous source term. The strong agreement between the Green's function and the molecular wave function [see the (2,27) state of Fig. 2] shows that this approximation is reasonable. The semiclassical Green's function at every point has been constructed from the coherent sum of four classical trajectories (see Fig. 5) in the Coulomb field. The semiclassical Green's function has only been shown up to the classical turning point where it diverges unphysically. The thin dark line on the  $z$  axis of the semiclassical Green's function is due to the numerical difficulty of integrating trajectories through the Coulomb singularity.

tori in phase space. Semiclassical quantization of these systems can be carried out through the Einstein-Brillouin-Keller (EBK) method [17,20], which quantizes the classical action of the trajectories on the tori according to the relation

$$\oint_{C_i} \vec{p} \cdot d\vec{r} = 2\pi \left( n_i + \frac{\mu_i}{4} \right), \quad (4.1)$$

where  $C_i$  is any closed loop and  $\mu_i$  is an integer that counts the number of conjugate points along the trajectory. At the quantized energies, this procedure selects a subset of all the trajectories in phase space. Every orbit in this subset of trajectories, which we will call the ‘‘EBK orbits,’’ then has the same quantized classical action. Our semiclassical approach follows this EBK method with one important modification that is motivated by the success of the Green’s-function approach in the previous section. Instead of considering all EBK orbits that satisfy Eq. (4.1), we consider only those that pass through the delta function perturbation associated with the ground state Rb atom at the point  $(\rho, z) = (0, R)$ . In this manner, we take the effect of the ground-state Rb atom into account. Put another way, we perform a constrained version of EBK quantization and only consider orbits that pass through the perturbing Rb atom. While this approach will not yield quantitative wave functions like degenerate perturbation theory, many of the qualitative features of the molecular wave functions will acquire simple semiclassical interpretations. Additional insight is also gained into why elliptic coordinates provide a simplified treatment of this problem.

A transformation of the classical Hamiltonian to elliptic coordinates shows why this coordinate system is ideal for describing the molecular Rydberg states. Notice that throughout this section, the perturbation potential does not appear in the Hamiltonian as we take it into account as a constraint on the trajectories. The Coulomb Hamiltonian in elliptic coordinates has a fixed pseudoenergy and can be written as  $H = H_\xi + H_\eta = 0$ , where

$$H_\xi = \frac{1}{2} p_\xi^2 (\xi^2 - 1) - \frac{R}{2} \xi - \frac{R^2}{4} E \xi^2, \quad (4.2)$$

$$H_\eta = \frac{1}{2} p_\eta^2 (1 - \eta^2) + \frac{R}{2} \eta + \frac{R^2}{4} E \eta^2. \quad (4.3)$$

In elliptic coordinates, the perturber is located at the point  $(\xi, \eta) = (1, 1)$ . When we constrain all of the classical trajectories to go through this point, we see that the value of the elliptic separation constant  $E_\xi$  is fixed at the value

$$E_\xi = -\frac{R}{2} - \frac{R^2}{4} E. \quad (4.4)$$

This is a unique property of elliptic coordinates for the Coulomb Hamiltonian, and gives insight into why the full molecular Hamiltonian has a preference for elliptic coordinates. In the other coordinate systems (spherical, parabolic) that the Coulomb potential is separable in, each trajectory that is constrained to pass through the perturber has a different value of the constant of the motion appropriate for that coordinate system. Thus, in spherical coordinates, each Coulomb ellipse that passes through the perturber at a fixed energy has a different value of the orbital angular momentum. Figure 7 illustrates this by showing a family of Coulomb ellipses in cylindrical coordinates. Each of the classical orbits has been constrained to pass through the perturber at  $(\rho, z) = (0, 1234)$  and it is apparent that every one has a different ellipticity and angular momentum. What is initially

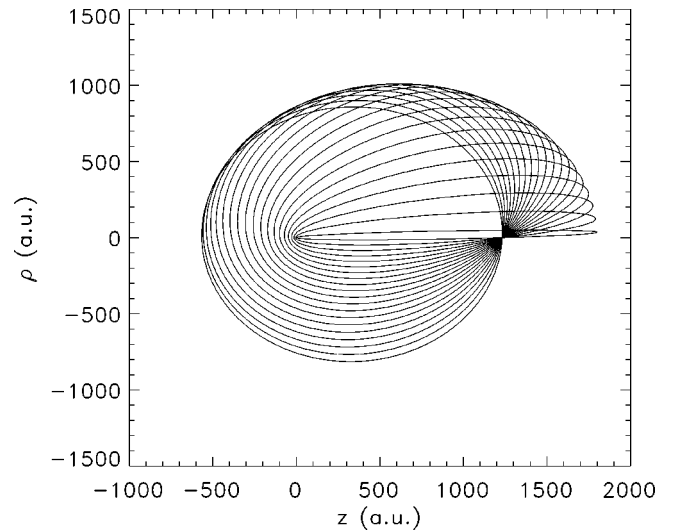


FIG. 7. A continuous family of elliptical trajectories for the Coulomb Hamiltonian. Each of these trajectories is an EBK orbit in elliptic coordinates and passes through the second focus of the elliptic coordinate system  $(\rho, z) = (0, 1234)$ . Even though each trajectory has a different value of the angular momentum and ellipticity, each one has the same value of the elliptic separation constant of Eq. (4.4).

hidden is that each of these orbits has the same value of the elliptic separation constant  $E_\xi$  given by Eq. (4.4). Classically, the generator of this rotation plus deformation of the Coulomb ellipses can be expressed in terms of the orbital angular momentum  $\vec{L}^2$  and Runge-Lenz vector  $\vec{A}$ . If  $\vec{R}$  is a vector pointing from the origin to the other focus (where the ground-state Rb atom would be), the elliptic constant of the motion  $E_\xi$  is related to the other constants of motion  $(E, \vec{L}^2, \vec{A})$  through the relation

$$E_\xi + E = \frac{4}{R^2} (\vec{R} \cdot \vec{A} - \vec{L}^2).$$

This relationship holds true even for trajectories that do not pass through the perturbing atom. This unique property of elliptic coordinates means that an efficient way of getting the excited electron to the attractive ground-state Rb atom is to fix the value of the elliptic constant of the motion. This yields intuitive insight as to why elliptic coordinates are preferred over the other possible coordinate systems for this problem.

To proceed with the semiclassical analysis, classical action variables associated with  $\xi$  and  $\eta$  motion are defined as  $J_\xi(E, E_\xi, R) = (1/2\pi) \oint p_\xi d\xi$  and  $J_\eta(E, E_\eta, R) = (1/2\pi) \oint p_\eta d\eta$ . The key point is that instead of proceeding with traditional EBK quantization, we include the effect of the perturber by requiring that all of the classical trajectories pass through the perturber  $(\xi, \eta) = (1, 1)$ . With this constraint, the action variables no longer depend independently on the separation constant  $E_\xi$  and the internuclear separation  $R$ , but only on the internuclear separation  $R$ . The constraint is implemented by setting the elliptic separation constant in the action variable to the constrained value of Eq. (4.4). Conve-

niently, the constraint allows analytical expressions for the “constrained” action variables to be found,

$$J_{\xi}(E,R) = \frac{1}{\sqrt{-2E}} - \frac{1}{\pi} \sqrt{2R(1+RE)} - \frac{1}{\pi} \sqrt{\frac{2}{|E|}} \arcsin \sqrt{|RE|}, \quad (4.5)$$

$$J_{\eta}(E,R) = \frac{1}{\pi} \sqrt{2R(1+RE)} + \frac{1}{\pi} \sqrt{\frac{2}{|E|}} \arcsin \sqrt{|RE|}. \quad (4.6)$$

We now use an EBK-type analysis to give two interpretations of these constrained action variables. The first interpretation involves defining effective quantum numbers based on the constrained action variables of Eqs. (4.5),(4.6). These effective quantum numbers then give information about the nodal structure in the molecular wave functions. The second interpretation proceeds with fixing the effective quantum numbers to be integers and finding quantized values of the total energy and internuclear radius. The quantized values of the internuclear radius will coincide with the minima of the full Born-Oppenheimer potential curves.

In standard EBK quantization, the action variables  $J(E)$  are related to the quantum numbers  $n$  in each degree of freedom through the relation  $J(E) = n + \mu/4$ , where  $\mu$  is the Maslov index. Thus, in a semiclassical picture we can regard the quantities

$$\nu_{\xi}(R) = J_{\xi}(E,R) - \frac{\mu}{4}, \quad (4.7)$$

$$\nu_{\eta}(R) = J_{\eta}(E,R) - \frac{\mu}{4}, \quad (4.8)$$

as the number of excitations (effective quantum numbers) in the  $\xi$  and  $\eta$  directions, as functions of the continuous variables  $(E,R)$ . In combination with Eqs. (4.5) and (4.6), Eqs. (4.7) and (4.8) give analytical expressions for the numbers of nodes in the full molecular wave function as functions of  $R$ . Figure 8 plots the resulting effective quantum numbers  $\nu_{\xi}(R)$  and  $\nu_{\eta}(R)$  for an  $n=30$  Rydberg state as a function of internuclear separation  $R$ . While it is difficult to obtain precise values of these effective quantum numbers for the full molecular state, rough estimates show that the semiclassical values shown in Fig. 8 agree well with the values of the full molecular wave functions of Fig. 2. Additionally, using the semiclassical values from this constrained EBK analysis, it is trivial to show that the molecular constraint ( $\nu_{\xi} + \nu_{\eta} = n - 1$ ) on the effective quantum numbers is an exact relation in this semiclassical approximation. This gives a semiclassical explanation of the observation that the numbers of nodes in the angular and radial elliptic directions always add up to the principal quantum number of the unperturbed Rydberg state minus one.

Another way of looking at the semiclassical mechanics of this system, is to proceed with the standard EBK quantiza-

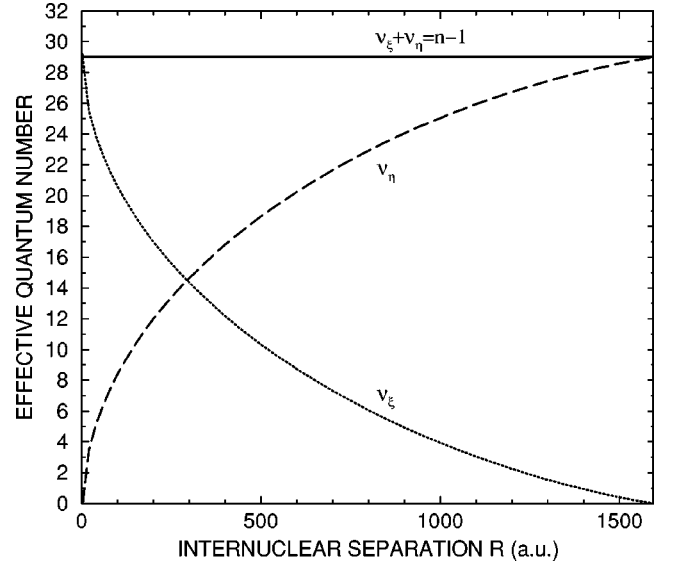


FIG. 8. The semiclassical effective quantum numbers  $\nu_{\xi}(R)$  and  $\nu_{\eta}(R)$  of Eqs. (4.7) and (4.8) for an  $n=30$  Rydberg state as a function of internuclear separation  $R$ . These effective quantum numbers characterize the nodal structure of the Born-Oppenheimer molecular states shown in Fig. 2. The underlying classical picture is that of classical trajectories of the Coulomb Hamiltonian that are constrained to pass through the perturbing Rb atom. This figure also shows that the sum of the effective quantum numbers is fixed at the value  $n - 1$ .

tion of the constrained action variables. This amounts to fixing the effective quantum numbers to integer values and solving Eqs. (4.7) and (4.8) for the quantized energies  $E$  and internuclear separations  $R$ . In the standard, unconstrained version of EBK quantization, the internuclear separation is not quantized, but remains a parameter of the elliptic coordinate system. In some sense, finding quantized values of  $R$  is artificial and unphysical. However, this constrained version of EBK quantization enables us to find a discrete set of internuclear separations for which *every* EBK orbit passes through the ground-state Rb atom. There are orbits that pass through the perturber at any value of  $R$ , but only at certain values of  $R$  are all of these orbits *also* quantized EBK orbits. To find the quantized values of  $R$  and  $E$ , we specify integer value  $(n_{\xi}, n_{\eta})$  and then find  $R$  and  $E$  numerically as the roots of Eqs. (4.7) and (4.8). This procedure yields the exact hydrogenic energies  $E_n = [-1/2(n_{\xi} + n_{\eta} + 1)^2]$  as well as a set of radii  $R_{min}^{EBK}$  shown in Table I. Table I also shows the values of the minima in the Born-Oppenheimer potential curve  $R_{min}^{BO}$  (Fig. 1) and demonstrates that the minima predicted by our constrained EBK quantization agree with the Born-Oppenheimer minima to within about 10 a.u. We believe that most of the discrepancy is due to the energy-dependent scattering length used to calculate the Born-Oppenheimer potential curve.

In this section, we have included the effect of the perturbing Rb atom in an unusual way. Rather than using the delta function interaction potential in the Hamiltonian, we include its effects through a constraint on the classical trajectories of the system. The advantage of this approach is that the



TABLE I. Positions of the minima in the Born-Oppenheimer potential curve  $R_{min}^{BO}$  are compared with separations  $R_{min}^{EBK}$  where every EBK orbit of elliptic coordinates passes through the perturbing Rb atom. Shown are the five outermost minima in the  $n=30$  potential curve. The good agreement (within about 10 a.u.) of the semiclassical EBK separations  $R_{min}^{EBK}$  with the minima  $R_{min}^{BO}$  in the Born-Oppenheimer potential curve shows that our constrained EBK analysis gives a reasonable semiclassical interpretation of the oscillations in the potential curve. Namely, that at the minima in the potential curve every EBK orbit of elliptic coordinates passes exactly through the perturbing Rb atom.

$(n_\xi, n_\eta)$	$R_{min}^{BO}$	$R_{min}^{EBK}$
(0,29)	1575	1597
(1,28)	1382	1389
(2,27)	1234	1234
(3,26)	1110	1106
(4,25)	1003	994

minima in the Born-Oppenheimer potential curves and the “quasiseparability” seen in degenerate perturbation theory obtain simple semiclassical interpretations. The quasiseparability (and minima in the potential curves) occurs when every EBK orbit in elliptic coordinates passes through the perturbing Rb atom. Our constrained EBK method also gives analytical semiclassical formulas for the effective quantum numbers that characterize the molecular states.

## V. CONCLUSION

In this paper we have investigated the properties of the electronic wave function and the Born-Oppenheimer potential curve of  $Rb_2$  Rydberg molecules. After the Born-

Oppenheimer Hamiltonian is transformed to elliptic coordinates, a simple picture of the molecular physics emerges. In this picture, the nature of the molecular state is determined by two ingredients. First, over most of configuration space, the molecular electron sees a pure Coulomb potential. In both our quantum and semiclassical treatments, the Coulomb physics in elliptic coordinates provides the starting point for understanding the molecular states. The second feature is the net attraction that the electron experiences when it gets near the ground-state Rb atom. If the Rydberg electron can spend most of its time nearby the ground-state Rb atom, this attraction will lead to a bound molecule.

Both in the quantum and semiclassical analysis, the role of elliptic coordinates is to concentrate the Rydberg electron at the position of the perturbing Rb atom. In the quantum case, we have shown that stationary, elliptic eigenstates of hydrogen accomplish this task efficiently. So much so, that at certain internuclear separations, a single elliptic state of hydrogen dominates the molecular wave function.

In the semiclassical case, we have shown that infinitely many classical Coulomb trajectories can be made to pass through the perturbing Rb atom by fixing the value of the elliptic constant of the motion. By incorporating these constrained Coulomb orbits into a semiclassical Green’s-function and an EBK style analysis, the elliptic nodal structure of the electronic wave function can be predicted semiclassically.

## ACKNOWLEDGMENTS

The work of B.E.G was supported in part by the U.S. Department of Energy, Office of Basic Energy Science. The work of E.L.H and C.H.G was supported by a grant from the National Science Foundation. We also benefited from discussions with A.S. Dickinson and H.R. Sadeghpour.

- 
- [1] C.H. Greene, A.S. Dickinson, and H.R. Sadeghpour, Phys. Rev. Lett. **85**, 2458 (2000).
  - [2] B. R. Judd, *Angular Momentum Theory for Diatomic Molecules* (Academic Press, New York, 1975).
  - [3] M.P. Strand and W.P. Reinhardt, J. Chem. Phys. **70**, 3812 (1979).
  - [4] P.D. Robinson, Proc. Phys. Soc. London **71**, 828 (1958).
  - [5] N.Y. Du and C.H. Greene, Phys. Rev. A **36**, 971 (1987).
  - [6] C. Bahrim and U. Thumm, Phys. Rev. A **61**, 022722 (2000).
  - [7] R.W. Molof, H.L. Schwartz, T.M. Miller, and B. Bederson, Phys. Rev. A **10**, 1131 (1974).
  - [8] S. Watanabe and C.H. Greene, Phys. Rev. A **22**, 158 (1983).
  - [9] Y. N. Demkov and V. N. Ostrovskii, *Zero-Range Potentials and Their Applications in Atomic Physics* (Plenum Press, New York, 1988).
  - [10] C.A. Coulson and P.D. Robinson, Proc. Phys. Soc. London **71**, 815 (1958).
  - [11] S.M. Sung and D.R. Herschbach, J. Chem. Phys. **95**, 7437 (1991).
  - [12] A. Sommerfeld, in *Atomic Structure and Spectral Lines*, 3rd ed. (Methuen and Co. Ltd., London, 1934), Chap. 2, pp. 116–119, as an historical note, the separability of the hydrogen atom in elliptic coordinates was not mentioned in the first two English editions of the text.
  - [13] H.A. Erikson and E.L. Hill, Phys. Rev. **75**, 29 (1949).
  - [14] Y. Duan and J.M. Yuan, Eur. Phys. J. D **6**, 319 (1999).
  - [15] C.A. Coulson and A. Joseph, Int. J. Quantum Chem. **1**, 337 (1967).
  - [16] M. C. Gutzwiller, *Chaos in Classical and Quantum Mechanics* (Springer-Verlag, New York, 1990).
  - [17] A. M. Ozorio de Almeida, *Hamiltonian Systems: Chaos and Quantization* (Cambridge University Press, Cambridge, 1988).
  - [18] L. Hostler, J. Math. Phys. **5**, 591 (1964).
  - [19] L. Hostler, J. Math. Phys. **8**, 642 (1967).
  - [20] M. Brack and R. K. Bhaduri, *Semiclassical Physics* (Addison-Wesley, Reading, MA, 1997).